

A 2D Numerical Simulation of Rayleigh-Bénard Convection at Varying Rayleigh Numbers with the Dedalus Project

Guilherme H. Caumo (260964615), Maryn Askew (260976675),
Sloane Sirota (261003293)

December 6, 2023

Abstract

This study developed a 2D numerical simulation for the fluid phenomenon of the Rayleigh-Bénard convection (RBC) with no-slip boundaries through pseudo-spectral methods. The study utilized Dedalus, a Python-based partial differential equation (PDE) solver, to compute the numerical simulation. We used the relative error between the Nusselt numbers on the top and bottom layers at varying Rayleigh numbers as a check for energy conservation, as the Nusselt number values should be identical in a physical system. Thereafter, the simulation was executed for Rayleigh numbers that had identical Nusselt numbers in the top and bottom convection layers to prevent large errors from dominating the run. Based on this, we observed that the 2D numerical RBC simulation behaved as expected within the selected domain, with numerical instabilities arising for Rayleigh numbers around $Ra = 10^8$. Overall, this study successfully characterized the properties of RBC using a 2D numerical simulation. Future studies should aim to implement computational methods that are able to function at higher Rayleigh numbers without facing numerical instabilities while also adding more physical characteristics to increase the power of the simulation.

1 Introduction

1.1 Theory and Equations

The RBC is a fundamental fluid dynamics problem that arises from a temperature imbalance between the top and bottom boundaries of a fluid's container (1). With a hotter bottom boundary and a cooler top boundary, the variation in density causes the heated fluid to rise while the cooled fluid descends, creating a circulation pattern. The Rayleigh number refers to the amount of convection in a system, where the Rayleigh number Ra is defined as

$$Ra = \frac{\alpha g \Delta T H^3}{\nu \kappa}, \quad (1)$$

where α is the thermal expansion coefficient, g is the gravitational acceleration, H is the thickness of the fluid layer, ν is the kinematic viscosity, κ is the thermal diffusivity of the fluid, and ΔT is the temperature difference between the top and bottom layers. The Prandtl number is defined as

$$Pr = \frac{\nu}{\kappa}. \quad (2)$$

Depending on the environmental parameters surrounding the fluid, there exists a critical number Ra_{crit} where the transition of there only being conduction within the fluid to there being advection present is observed. As the Rayleigh number becomes higher, more heat is transported by advection, and the convection becomes increasingly turbulent (i.e. the fluid layers begin interacting). From Eq.1, we see that increased fluid density results in a higher Ra , thus increasing the possibility of turbulent convection.

Concurrently, the Navier-Stokes equations are a set of PDE's describing the motion of a viscous fluid. The Navier-Stokes expression for conservation of momentum of an incompressible, Newtonian fluid is

$$\frac{\partial \mathbf{u}}{\partial t} + (\mathbf{u} \cdot \nabla) \mathbf{u} - \nu \nabla^2 \mathbf{u} = -\frac{1}{\rho} \nabla p + \mathbf{g}, \quad (3)$$

where \mathbf{u} is the flow velocity, ρ is the mass density, p is the pressure, ν is the kinematic viscosity, and \mathbf{g} represents the body accelerations acting on the fluid. The Boussinesq approximation is a simplification applied to the Navier-Stokes equations, which assumes that the density variations in the fluid are small except for a buoyancy term due to temperature differences. The non-dimensional Oberbeck-Boussinesq equations modelling RBC can be written as

$$\frac{1}{Pr} \left(\frac{\partial \mathbf{u}}{\partial t} + \mathbf{u} \cdot \nabla \mathbf{u} \right) = -\nabla p + Ra T \cdot \hat{z} + \nabla^2 \mathbf{u}, \quad (4)$$

$$\nabla \cdot \mathbf{u} = 0, \quad (5)$$

$$\frac{\partial T}{\partial t} + \mathbf{u} \cdot \nabla T = \nabla^2 T. \quad (6)$$

Considerable attention has been devoted to understanding the dynamics of fluid convection at elevated Rayleigh numbers. This research is of significance due to the prevalence of high Rayleigh numbers in various fields, including geophysics, atmospheric science, and engineering (2) (3). It is believed that there are distinct scaling regimes that exist for different ranges of Ra , prompting extensive investigations to obtain the precise scaling of the Nusselt number Nu . The Nusselt number can be described as an average over a domain. Using a volume integral, this can be written as

$$Nu = \frac{1}{V} \int_V \left(-\frac{\partial T}{\partial t} + u_z T \right) dV, \quad (7)$$

where V is the volume, and u_z is the vertical component of the velocity field. By conservation of energy, it follows that the Nusselt numbers calculated at the top and bottom of the domain should be equal to each other (4), which has been used as a consistency check in the literature (5)(6).

1.2 Problem Description

In this work, the Dedalus Python package is used to simulate 2D RBC using pseudo-spectral methods. We aim to observe how the fluid dynamics are affected by varying Ra while $Pr = 1$. We use fixed temperatures at the bottom plate ($T = 1$) and top plate ($T = 0$) and implement no-slip boundaries into the simulation. To verify the consistency of the simulation, we checked whether energy was conserved in the simulated system by calculating the relative error of Nusselt numbers calculated at the top and bottom layers in the convection, which should be identical (4). By accurately simulating the RBC, this project is pertinent to general problems involving fluid dynamics in astrophysics and geophysics (2) (3).

2 Methodology

2.1 Code Description

To simulate RBC in two dimensions, we use the powerful PDE solver Python package, Dedalus (7), which presents an example script named “raleigh_benard.py” that uses Boussinesq approximations to the Navier-Stokes equations in a 2D Cartesian domain. Space is discretized by Dedalus’ pseudo-spectral method, using Fourier bases with periodic boundaries in the horizontal x-direction, and Chebyshev polynomial bases for the vertical z-direction. The example script begins by setting up the parameters such as simulation time, box dimensions (L_x , L_z) and grid resolution (N_x , N_z), the Rayleigh numbers that we vary, and the Prandtl numbers, which we hold constant at $Pr = 1$ for this study. The non-dimensionalization is done using box height and freefall time, and thermal diffusivity “kappa” and viscosity “nu” are defined based on the Rayleigh and Prandtl numbers. Below is an example of how Dedalus’ framework defines the fields for pressure p , buoyancy b , and velocity u , including various “tau” terms.

```
# Fields
p = dist.Field(name='p', bases=(xbasis, zbasis))
b = dist.Field(name='b', bases=(xbasis, zbasis))
u = dist.VectorField(coords, name='u', bases=(xbasis, zbasis))
tau_p = dist.Field(name='tau_p')
tau_b1 = dist.Field(name='tau_b1', bases=xbasis)
tau_b2 = dist.Field(name='tau_b2', bases=xbasis)
```

```
tau_u1 = dist.VectorField(coords, name='tau_u1', bases=xbasis)
tau_u2 = dist.VectorField(coords, name='tau_u2', bases=xbasis)
```

One of the most powerful aspects of Dedalus is the introduction of tau terms which are used to stabilize the numerical solution of the PDEs. Instead of directly solving for the spatial gradients in the PDEs, the code introduces auxiliary variables like “tau_u1” and “tau_b1”, which represent the first-order spatial gradients of the velocity and temperature fields. First-order formulation is used for the auxiliary variables, as illustrated in the substitutions portion of the code below. For instance, “grad_u” and “grad_b” are defined in terms of “tau_u1” and “tau_b1” respectively. Here the script is able to use a first-order reduction technique to express the PDE’s in terms of first-order spatial derivatives.

```
# Substitutions
kappa = (Rayleigh * Prandtl)**(-1/2)
nu = (Rayleigh / Prandtl)**(-1/2)
x, z = dist.local_grids(xbasis, zbasis)
ex, ez = coords.unit_vector_fields(dist)
lift_basis = zbasis.derivative_basis(1)
lift = lambda A: d3.Lift(A, lift_basis, -1)
grad_u = d3.grad(u) + ez*lift(tau_u1) # First-order reduction
grad_b = d3.grad(b) + ez*lift(tau_b1) # First-order reduction
```

The script then defines the problem as an initial value problem using the “d3.IVP” class and equations are added using “add.equation,” which includes conservation of momentum, the Navier-Stokes equations after substitutions, no-slip boundary conditions, and fixed buoyancy, which relates directly to temperatures of $T = 1$ at the bottom plate and $T = 0$ at the top plate. Initial conditions are also included where random noise is added to the temperature with damping at the walls, and a linear background is implemented. After the problem is defined, a solver is created using a general implicit-explicit Runge-Kutta time-stepping scheme. In the code, the CFL (named after Courant-Friedrichs-Lewy) class from Dedalus is applied to control the time step and adapt it to ensure numerical stability. Finally, there is a main loop at the end of the script that iteratively advances the solution in time until the specified stop time.

2.2 Code Tests and Analysis

After the simulation is run for different values of Ra , we plot the steady state temperature fields and Nusselt number Nu as well as its error as a function of Ra in another notebook labelled as “Figs.ipynb”. The horizontally averaged temperature profile for different orders of magnitude is included to show how the temperature gradient strays away from a linear background when only conduction is present as Ra is increased and advection is introduced to the system.

To evaluate whether the RBC simulation is accurate, the Nusselt number was evaluated in the top and bottom plates of the convection. Within the example script, we add a simple calculation through Eq.7, using built-in functions within Dedalus like “d3.Differentiate” to compute the partial derivative of the temperature gradient with respect to z and taking the horizontal average using “d3.Average”. Dedalus allows for saving data using a file handler where we compile files with a maximum of 400 writes for which we access later via HDF5 files using the h5py library to obtain necessary data on fields recorded by “solver.state” and the Nusselt numbers for steady state solutions. Below is a snippet of code showing the method used by Dedalus to save tasks for analysis.

```

# keep track of nusselt number and field evolution
analysis = solver.evaluator.add_file_handler('analysis', iter=10,
                                             max_writes=400)

# partial derivative with respect to z
dz = lambda A: d3.Differentiate(A, coords['z'])
analysis.add_task(d3.Average(-dz(b), 'x'), layout='g',
                  name='Nusselt-Number')
analysis.add_tasks(solver.state, layout='g')

```

Based on the law of conservation of energy, the Nusselt number on top, Nu_t , must be equal to the Nusselt number on the bottom, Nu_b (4). Figure 1 shows the relative error of the top and bottom Nusselt numbers for multiple runs with varying Rayleigh numbers. From Figure 1, we observe that Rayleigh numbers at the order of 10^8 lead to large errors as the relative error between the top and bottom Nusselt numbers becomes non-zero. This indicates that conservation of energy breaks down at that Rayleigh number scale. This is due to the simulation being computationally expensive, so the Dedalus-based algorithm fails to run efficiently and the run breaks down. Figure 2 shows the value of the averaged top and bottom Nusselt number evaluated at multiple scales of the Rayleigh number.

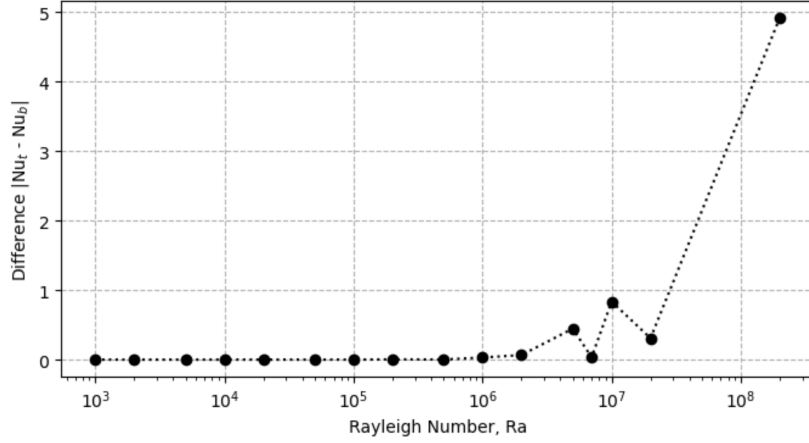


Figure 1: Relative error of Nusselt number taken on top and bottom of convection cell plotted with respect to Rayleigh number.

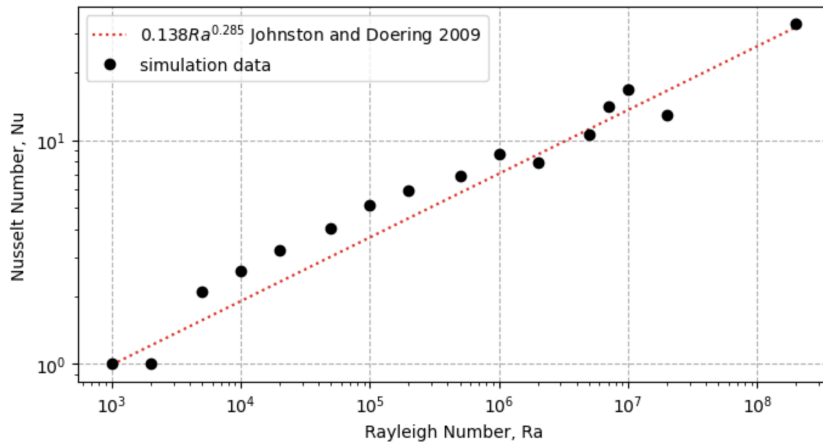


Figure 2: Average value of Nusselt number from top and bottom values plotted with respect to Rayleigh number.

We do a consistency check with Johnston and Doering’s empirical scaling for the Nusselt number, which found that $Nu = 0.138Ra^{0.285}$ (4). For Ra from 10^3 to 10^6 , there is a curve that does not match the scaling but after about 10^6 , the data converges to the scaling. This behavior is similar to the behavior found in (8).

3 Result and Analysis

The RBC simulation is shown in Figure 3. The figure depicts a clear, physical pattern from the numerical RBC simulation with the scaling of the Rayleigh number. Under the influence of a small Rayleigh number, $Ra = 10^3$, only conduction is present in the system so the initial temperature gradient is observed. By increasing the Rayleigh number, the critical number is surpassed and advection is introduced to the system, defined as the movement of fluid due to velocity for Rayleigh number values $Ra = 10^4, 10^5, 10^6$ and 10^7 . At $Ra = 10^8$, the simulation of the temperature field starts to break down, resulting in numerical instability which causes violations in conservation of energy as evident by the errors in Figure 1. Figure 4 shows the horizontally averaged temperature for varying Rayleigh numbers becoming less linear for increasing Rayleigh number scales, and becoming less smooth for high Rayleigh number scales. The instability of the simulation can more easily be seen in the “movies” folder as the simulation runs more smoothly for lower orders of magnitude, and less smoothly for higher orders of magnitude.

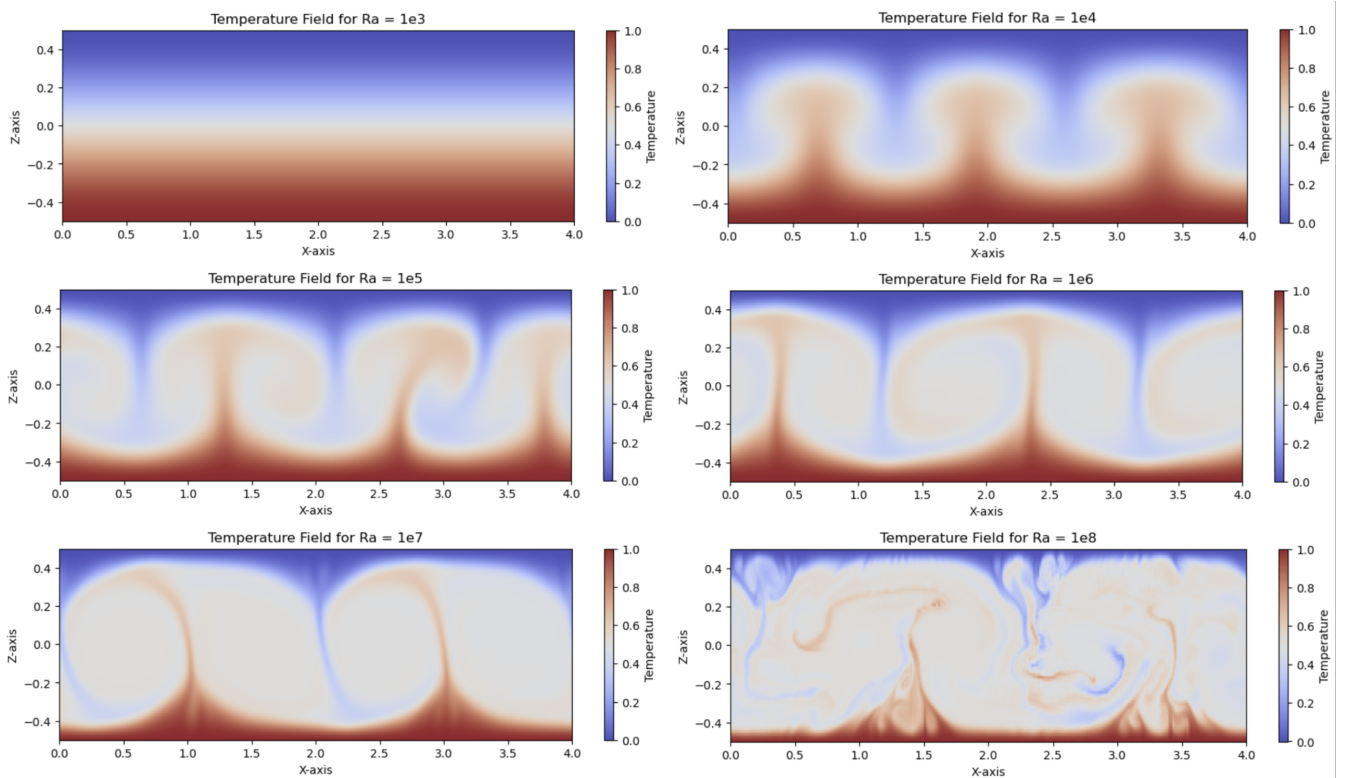


Figure 3: RBC temperature field depicted for increasing values of Rayleigh numbers at $Ra = 10^3, 10^4, 10^5, 10^6, 10^7$, and $Ra = 10^8$ after enough time for a steady state to be reached. The bottom plate is fixed at $T = 1$, whilst the top plate is fixed at $T = 0$, and both top and bottom plates are no-slip while there are periodic horizontal boundaries.

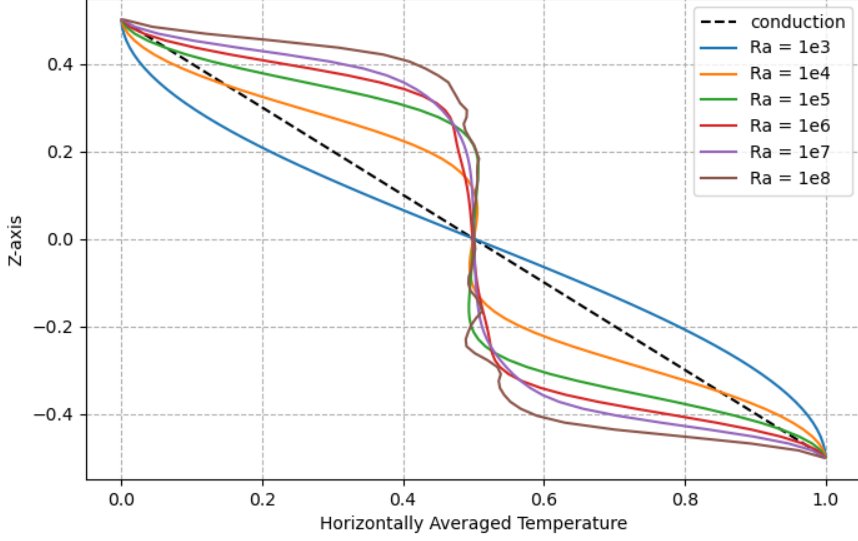


Figure 4: Horizontally averaged temperature for increasing values of Rayleigh numbers at $Ra = 10^3, 10^4, 10^5, 10^6, 10^7$, and $Ra = 10^8$, dotted line represents the initial linear temperature gradient indicating that theoretically, only conduction would be present. Once the temperature profile significantly strays from linear, we have advection present.

4 Discussion and Further Improvements

Based on Figure 3 and Figure 4, it is possible to state that the 2D numerical simulation for the RBC is successfully produced with no-slip boundary conditions through the pseudo-spectral methods. For no-slip conditions, we should see a critical number of $Ra \approx 1700$ for where the simulation transitions from only conduction being present, to having advection (1). This can be seen between the first two plots in Figure 3. As the Rayleigh number increases in orders of magnitude, there comes a point where the simulation becomes numerically unstable at $Ra = 10^8$, which is demonstrated by the relative error of the Nusselt number in Figure 1. The results from Figure 3 are also illustrated by Figure 4, where the horizontally averaged temperature strays further from the linear conduction by increasing the Rayleigh number. Furthermore, Figure 4 demonstrates that for large Rayleigh number scales the temperature gradients not only stray far from the initial linear temperature gradient that represents conduction but also become less smooth due to increasingly turbulent flow.

It is important to note that this code can be improved by implementing a numerical scheme capable of simulating larger Rayleigh numbers, as the simulation does introduce large errors starting at $Ra = 10^8$. This can be achieved by optimizing the program so it is less computationally expensive at larger values, or running the simulation in parallel as demonstrated in other literature (8), where simulations that scale up to $Ra = 10^{10}$ have been achieved. However, for the purposes of this study, the 2D simulation achieves success in simulating RBC within a reasonable range. Another improvement of interest would be implementing a third dimension to the simulation, as an accurate 3D numerical simulation for RBC could be used to examine fluid dynamics with even more depth. Finally, the numerical simulation can be extended further by introducing more complex physical effects and adjust it to suit specific systems, such as astrophysical or geophysical systems that are well understood in the literature (2) (3), to verify the efficiency of the simulation and its capacity to explain fluid dynamics in multiple settings.

5 Conclusion

It is possible to conclude that the 2D numerical simulation successfully characterized the properties of RBC for the domain $Ra < 10^8$. By accurately simulating the temperature fields for RBC at varying Rayleigh numbers, this study shows excellent capacity in demonstrating fluid dynamics through pseudo-spectral methods. Furthermore, this study successfully characterizes the behaviour of the simulation in regions where errors are introduced by testing for the conservation of energy comparing the top and bottom Nusselt numbers in the convection. Future studies should consider improving the methods presented here by implementing computational methods that are able to function at higher Rayleigh numbers without facing numerical instabilities while also adding more physical characteristics to increase the power of the simulation.

6 Acknowledgements

The authors of this project all contributed equally, and participated in the research, coding, and writing of this paper. The authors would also like to express their gratitude to Professor Andrew Cumming for his recommendation of the Dedalus Project, which provided a much needed backbone to the computational methods applied here.

References

- [1] G. Ahlers, S. Grossmann, and D. Lohse, “Heat transfer and large scale dynamics in turbulent Rayleigh-Bénard convection,” *Rev.Mod.Phys*, vol. 81, no. 2, 2009.
- [2] F. H. Busse, “Non-linear properties of thermal convection,” *Rep. Prog. Phys.*, vol. 41, no. 12, 1978.
- [3] J. Olsthoorn, “Accounting for surface temperature variations in Rayleigh-Bénard convection,” *Phys. Rev. Fluids*, vol. 8, no. 3, 2023.
- [4] H. Johnston and C. R. Doering, *A comparison of turbulent thermal convection between conditions of constant temperature and constant heat flux boundaries*, Eckhardt, B. (eds) Advances in Turbulence XII. Springer Proceedings in Physics, vol 132. Springer, Berlin, Heidelberg, 2009.
- [5] E. King, S. Stellmach, and B. Buffett, “Scaling behaviour in Rayleigh-Bénard convection with and without rotation,” *Journal of Fluid Mechanics*, vol. 717, pp. 449-471, 2013.
- [6] J. Mound and C. Davies, “Heat transfer in rapidly rotating convection with heterogeneous thermal boundary conditions,” *Journal of Fluid Mechanics*, vol. 828, pp. 601-629, 2017.
- [7] K. J. Burns, G. M. Vasil, J. S. Oishi, et al. “Dedalus: A flexible framework for numerical simulations with spectral methods,” *Phys. Rev. Research*, vol. 2, no. 2, 2020.
- [8] A. Clarke, C. Davies, D. Ruprecht, et al. “Performance of parallel-in-time integration for Rayleigh Bénard convection,” *Comput. Visual Sci.*, vol. 23, no. 10, 2020.